Journal of Physics: Conference Series **2429** (2023) 012025 doi:10.1088/1742-6596/2429/1/012025

High-energy neutrino astronomy — the neutrino connections to the cosmic-ray origin: present and future

Shigeru Yoshida

International Center for Hadron Astrophysics, Chiba University, Chiba 263-8522, Japan

E-mail: syoshida@hepburn.s.chiba-u.ac.jp

Abstract. High-energy neutrino astronomy has been blooming. In addition to the possible identification of the blazar and Seyfert II galaxies as neutrino emitters, the present neutrino data has indicated some hints to characterize or constrain the origin of cosmic rays. Being motivated by the observational fact that the astrophysical neutrino background energy flux is comparable to that of ultrahigh-energy (UHE) cosmic rays, we derive the generic requirements that a major fraction of UHE cosmic ray sources must meet, if they are also responsible for the ~ 100 TeV-energy cosmic neutrino background radiation. The source parameters characterizing the cosmic ray – neutrino unified scheme, such as the photon radiation luminosity and the cosmic ray luminosity density, suggest that the yet-unidentified cosmic ray and neutrino origins can be transient objects visible in the optical/NIR wavelength band. We propose a viable scheme of multimessenger observations to identify the sources using the neutrino multiplet detections.

1. Introduction

The discovery of high-energy cosmic neutrinos has provided information useful for understanding how the universe produces UHE cosmic rays (UHECRs). Since neutrinos are electrically neutral and only weakly interacting, their directions and timing profiles can reveal their sources. Moreover, the observations of the flux of astrophysical neutrino background radiation, the quasi-isotropic radiations superposing the individual emissions from numerous neutrino sources distributed over cosmological distances, are quite informative to understand the UHECR origin. As shown in the left panel of Figure 1, the energy flux of the neutrino background radiation, $E_\nu^2\Phi_\nu$, is $O(10^{-8})$ GeV cm^{-2} sec^{-1} sr^{-1} at ~ 100 TeV energies, which is comparable to that of UHECRs. This possibility had been predicted [1] and has been further discussed [2] in the literature. If there are indeed connections between UHECRs and the high-energy neutrinos the IceCube observatory has been measuring, the flux compatibility is not surprising, given that the UHECR sources meet some criteria. We will discuss them in some details in this paper.

Having a closer look at the cosmic neutrino background flux data presented in the right panel of Figure 1, one can notice that the flux below 30 TeV seems to reach $O(10^{-7})$ GeV cm^{-2} sec^{-1} sr^{-1}, which is significantly higher than the UHRCR flux. Such high neutrino fluxes cannot be directly connected to UHECRs nor GeV-energy gamma rays, if the power-raw like spectrum is continuing down to $E \ll$ TeV. It is rather likely that the sources radiating TeV-energy neutrinos are optically (and hadronically) thick, which implies that any direct connections to the observed UHECRs and GeV gamma-rays cannot be realized[1]. Keeping this scenario in mind, we assume

[1] but the MeV-energy gamma rays can be highly relevant. See Ref [4] for example.

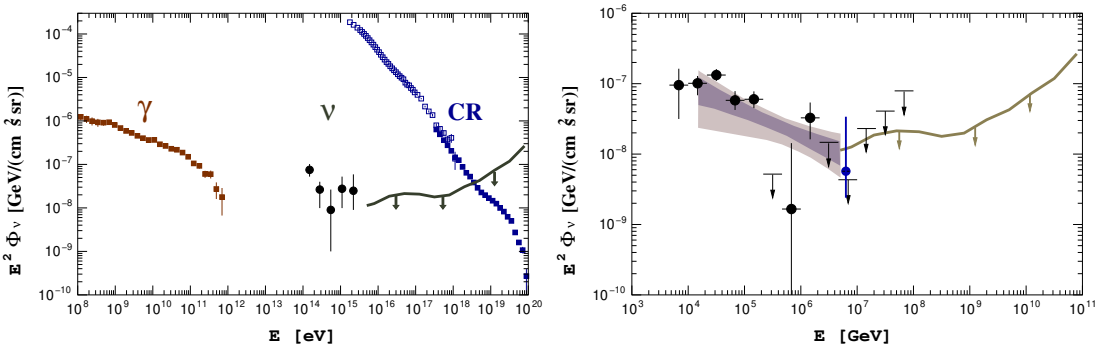

Figure 1. Left: The global energy spectrum of the cosmic background radiation in the energy region above 10^8 eV. Right: The spectrum of high-energy neutrino background radiation measured by the IceCube experiment. The most updated data available as of the time when this article was written participated the plot. The blue data point was obtained by the $\bar{\nu}_e$ detection via the Glasgow resonance [3]. All three neutrino flavor sum flux (converted from a single flavor data when necessary) is presented.

here that cosmic back ground neutrinos at energies above $\sim$ 100 TeV are different in origin. We should remark that, although the present data statistics cannot rule out the hypothesis that the whole neutrino spectrum simply follows a single power law, a log-parabolic or broken power law would describe the data better. A "two-component" neutrino scenario is, therefore, rather viable.

In a two-component model, the 2nd component at energies above 100 TeV may share its origin with UHECRs as we stated above. What are the general characters of these sources? The upper-limit of the neutrino flux above 10 PeV, the so called Extremely High-Energy (EHE) neutrino limit presented by the thick line in the right panel of Figure 1, has already set constraints on the source *evolution* factor. The sources must be objects that have evolved on time scales comparable to or slower than the star formation rate [5]. This was what we mainly argued in CRIS 2016. The pronounced EHE neutrino flux generated by the GZK mechanisms would not be avoidable, otherwise. A significant part of the parameter space in the models involving the radio-loud AGNs, new-born pulsars, and the classical gamma ray bursts (GRBs) seems unfavorable. This conclusion depends on the mass composition of UHECRs [6], but the neutrino stacking analyses using the GRB detection alerts and Fermi Blazar source catalog are also consistent with this picture. It is likely that the UHECR emitters are only weakly evolved.

In this article, we discuss what the UHECR sources must generally meet if they are also responsible for the neutrino sky at energies above $\sim$ 100 TeV, on top of the requirement that they cannot be strongly evolved in the redshift space. We present the parameter space allowing UHECRs and neutrinos to share the same origin particularly in the photo-meson production ($p\gamma$) scheme. The case of the hadronuclear (pp) framework was discussed elsewhere for example in Ref. [7]. Possible UHECR-neutrino sources viable in the $p\gamma$ scheme are transient in X-ray and optical/NIR bands, and conducting rapid followup multiwavelength observations is a key to identify such sources. However, the optical transient sky contains a full of supernovae (SNe) which makes it challenging to find the solid association between a neutrino signal and its optical counterpart candidate. We study a new strategy of realizing the robust multimessenger observations by searching for high-energy multiplet neutrino events with a 1 km^3 neutrino telescope. We present the sensitivity of the multiplet search and the tactics to identify a neutrino source by optical/NIR follow-up observations.

2. A generic unification model

We consider a generic scenario that the both UHECRs and high-energy neutrinos with $E_\nu \gtrsim 100$ TeV originates from the same astrophysical phenomena. We start with describing a source to generate UHECRs and neutrinos in comprehensive and generic ways, and introduce a set of parameterization for defining the UHECR and neutrino emission processes. Requirements for emitting UHECRs and neutrinos are derived using the introduced parameters. We also calculate their fluxes and compare them with the observational data to obtain further requirements the unified sources must meet. The details of the modeling and the relevant discussions are fully described in Ref. [8].

2.1. A source modeling

We construct a generic source model to emit both UHECRs and secondary neutrinos via the photo-meson production scheme. A cosmic ray acceleration region as well as an emission region are located at distance R from the central engine. A plasma flow with the bulk Lorentz factor Γ fills these regions. Variables in the plasma rest frame are denoted by prime ('). We introduce the six parameters as following:

- A bulk Lorentz factor of the plasma outflow in the CR acceleration (and neutrino production) site, Γ.
- A comoving radiation luminosity $L'_\gamma = L_\gamma/\Gamma^2$.
- The source number density in the local universe n_0.
- The optical depth of pγ interactions at the cosmic ray proton energy $\tilde{\varepsilon}_0 \equiv 10$ PeV, $\tau_{p\gamma 0}$.
- The equipartition parameter $\xi_{\rm B}$. $\xi_{\rm B} = 1$ when the B-field energy density balances to the photon radiation energy density.
- A cosmic ray loading factor $\xi_{\rm CR}$ to represent the ratio of the cosmic ray output power to the photon radiation luminosity.

In addition, the source evolution parameter $\psi(z)$ describes the evolution of the unified sources. As we described in Section 1, it must be weaker or comparable to the star formation rate (SFR). Here we set $\psi(z)$ to trace the SFR.

In most of the cases considering known astronomical objects, the spectrum of photons colliding to UHECR protons can be approximately described by a power law formula, $dn_\gamma/\varepsilon'_\gamma \propto (\varepsilon'_\gamma)^{-\alpha_\gamma}$, at least for the wavelength region where $p\gamma$ interactions matter. Then the $p\gamma$ optical depth is given by

$$\tau_{p\gamma}(\varepsilon_{\rm CR}) = \tau_{p\gamma 0}\left(\frac{\varepsilon_{\rm CR}}{\tilde{\varepsilon}_0}\right)^{\alpha_\gamma - 1}, \tag{1}$$

where the depth at energy of $\tilde{\varepsilon}_0 = 10$ PeV, $\tau_{p\gamma 0}$, is determined by the source radiation luminosity and the comoving B field as

$$\tau_{p\gamma 0} = \frac{B'}{\Gamma^2}\sqrt{\frac{L'_\gamma}{\xi_{\rm B}}}C(\alpha_\gamma, \tilde{\varepsilon}_0). \tag{2}$$

The equipartition principle via $\xi_{\rm B}$ eliminates the explicit appearances of the distance R here. The term C is a constant determined by the $p\gamma$ cross section $\sigma_{p\gamma}$ and the photon spectral index, and given by

$$C(\alpha_\gamma, \tilde{\varepsilon}^\Delta_{p0}) \sim 2.4\times10^{-24}\ {\rm erg}^{-1}\ {\rm cm}^{3/2}\ {\rm s}^{1/2}\left(\frac{2}{1+\alpha_\gamma}\right)\left(\frac{\tilde{\varepsilon}_0}{10\ {\rm PeV}}\right). \tag{3}$$

Note that the main energy of target photons for UHECR protons with energy of $\tilde{\varepsilon}_0 = 10$ PeV is determined by the Δ-resonance condition of the $p\gamma$ interactions, and obtained by

$$\varepsilon_{\gamma 0} \approx 16\ \Gamma^2(\tilde{\varepsilon}_0/10\ {\rm PeV})^{-1}\ {\rm eV}. \tag{4}$$

Thus the photons involving the neutrino production are in optical/UV ($\Gamma \sim 1$) or X rays ($\Gamma \sim 10$). Note that the photon luminosity of the source L'_γ is defined at this energy.

2.2. Requirements for emitting UHECRs and neutrinos

The UHECR acceleration condition requires their acceleration time scale to be faster than the dynamical time scale in the source system. It leads to the lower bound of the source photon luminosity as

$$\begin{aligned} L'_\gamma &\geq \frac{1}{2}\xi_B^{-1} c\eta^2\beta^2 \left(\frac{\varepsilon_{\rm CR}^{\rm max}}{Ze}\right)^2 \\ &\gtrsim 1.7\times 10^{45}\xi_B^{-1}\eta^2\beta^2 \left(\frac{\varepsilon_{\rm CR}^{\rm max}}{Z10^{11}\ {\rm GeV}}\right)^2\ {\rm erg/s} \quad . \end{aligned} \tag{5}$$

The escape condition demands UHECRs escape from the acceleration cite before being cooled down by the synchrotron radiation. It consequently limits the strength of B-field as

$$B' < \frac{6\pi A^4 m_p^4 c^{9/2}}{Z^4\sigma_T m_e^2 (2\xi_B L'_\gamma)^{1/2}} \frac{\Gamma^2}{\varepsilon_{\rm CR}^{\rm max}}. \tag{6}$$

This B-field limit essentially requires that the acceleration and the $p\gamma$ collision take place at reasonably far distances from the central engine. This constraint can be represented by the condition of the photo-meson optical depth as

$$\tau_{p\gamma 0} \lesssim 6\times 10^{-2}\frac{2}{1+\alpha_\gamma}\xi_B^{-1}\left(\frac{A}{Z}\right)^4 \left(\frac{\varepsilon_{\rm CR}^{\rm max}}{10^{11}\ {\rm GeV}}\right)^{-1}. \tag{7}$$

This bound indicates that the optical depth can be too small to make it visible in the neutrino sky unless $\xi_{\rm B} \ll 1$. We come back to discuss this point in the next section.

If the observed UHECRs bulk is dominated by nuclei rather than protons, the nuclear survival condition must be applied. The accelerated nuclei must get out of their sources before being completely broken down by the photodisintegration. This condition is represented by

$$\tau_{A\gamma}(\varepsilon_{\rm CR}^{\rm max}) \lesssim A, \tag{8}$$

where $\tau_{A\gamma}$ is the optical depth of the photodisintegration. Because we can relate $\tau_{A\gamma}$ to $\tau_{p\gamma 0}$, we obtain the bound of $\tau_{p\gamma 0}$ as

$$\begin{aligned} \tau_{p\gamma 0} &\lesssim A\frac{\int ds \frac{\sigma_{p\gamma}(s)}{s-m_p^2}}{\int ds \frac{\sigma_{A\gamma}(s)}{s-m_A^2}} \left[\left(\frac{s_{\rm GDR}-m_A^2}{s_\Delta - m_p^2}\right)\left(\frac{\tilde{\varepsilon}_0}{\varepsilon_{\rm CR}^{\rm max}}\right)\right]^{\alpha_\gamma - 1} \\ &\lesssim 0.4\left(\frac{A}{56}\right)^{0.79}. \end{aligned} \tag{9}$$

2.3. Requirements to explain the observed fluxes of UHECRs and neutrinos

With these conditions above, we can calculate the fluxes of UHECRs and neutrinos. Both the UHECR and the neutrino diffuse background fluxes scale as $\propto n_0\xi_{\rm CR}L_\gamma \approx n_0\xi_{\rm CR}L'_\gamma\Gamma^2$. It is convenient to introduce the *boosted* source number density defined as

$$\mathcal{N}_\Gamma \equiv n_0\xi_{\rm CR}\Gamma^2 = \rho_0\Delta T\xi_{\rm CR}\Gamma^2, \tag{10}$$

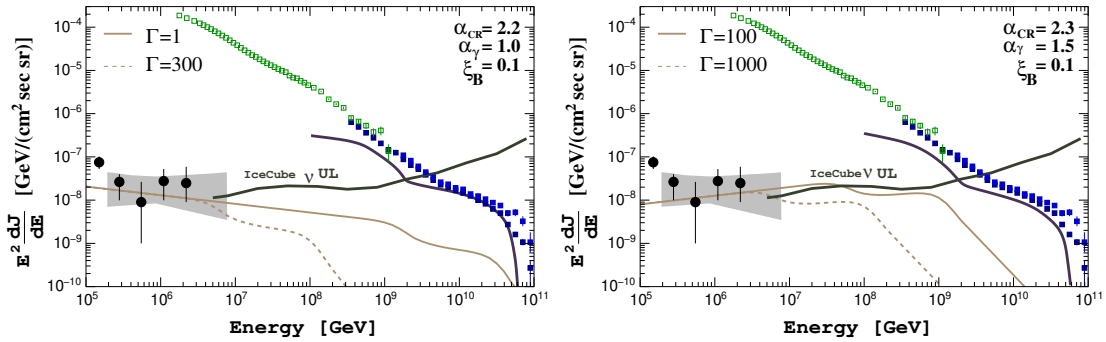

Figure 2. Left: An example of the UHECR nucleon and the all-flavor-sum neutrino fluxes from UHECR sources calculated by the present analysis. The case of $\alpha_{\rm CR} = 2.2$, $\alpha_\gamma = 1.0$, $\xi_{\rm B} = 0.1$ is shown. The comoving L'_γ is set to 4.5×10^{46} erg/s and the boosted source number density $\mathcal{N}_\Gamma$ (Eq. 10) is 1×10^{-9} Mpc^{-3}. The optical depth $\tau_{p\gamma 0}$ is 0.30 in this particular example, which gives the magnetic field of $B' = 0.91\Gamma^2$ G with $\xi_{\rm B} = 0.1$. The black points are the IceCube neutrino measurements [10] and the shaded region represents the flux space consistent with the IceCube diffuse ν_μ data [11]. The solid curve labeled by (IceCube ν UL) is the differential EHE bound by IceCube [12]. Right: An example of scenario for hard neutrino flux. $\alpha_{\rm CR} = 2.3$ and $\alpha_\gamma = 1.5$. The comoving L'_γ is set to 5.0×10^{48} erg/s and the boosted source number density $\mathcal{N}_\Gamma$ (Eq. 10) is 1×10^{-9} Mpc^{-3}. The optical depth $\tau_{p\gamma 0}$ is 0.10 in this particular example.

where ρ_0 is a density rate of flare with time scale of ΔT. The cosmic ray loading factor $\xi_{\rm CR}$ decides the UHECR background radiation intensity with reference to the source photon luminosity.

By the semi-analytical formulation to calculate the UHECR and the neutrino energy spectrum [8, 9], we obtained the allowed region of the parameter space in $\mathcal{N}_\Gamma, L'_\gamma, \tau_{p\gamma 0}$ by comparing the calculated spectra to the observational data, for a given set of the spectral power law indices of photons and UHECRS, α_γ and $\alpha_{\rm CR}$. An example of the UHECR and neutrino fluxes by the unified source population belonging in the allowed region of the parameter space is shown in the left panel of Figure 2.

The observed UHECR flux, and the observed flux and its upper limit of neutrinos lead to the following constraints. The $p\gamma$ optical depth must meet

$$0.1 \lesssim \tau_{p\gamma 0} \lesssim 0.6, \tag{11}$$

which turns into the upper bound of $\xi_{\rm B}$ via the UHECR escape condition, Eq. (7) as

$$\xi_{\rm B} \lesssim 0.5. \tag{12}$$

$\mathcal{N}_\Gamma$ and L'_γ are bounded to a narrow range for the UHECR and neutrino fluxes to reach to the observed intensity as shown in the left panel of Figure 3. This bound can be approximately described as

$$L'_\gamma \mathcal{N}_\Gamma = n_0 L'_\gamma \xi_{\rm CR} \Gamma^2 \approx (1-4) \times 10^{45} \text{ erg Mpc}^{-3} \text{ yr}^{-1}. \tag{13}$$

This bound weakly depends on the optical depth $\tau_{p\gamma 0}$ and the allowed region is presented in the right panel of Figure 3. With the UHECR escape and survival conditions, the only very narrow parameter space is allowed. It suggests that we can easily verify the UHECR-neutrino unified scenario by future observations.

The falloff of the neutrino spectrum at the highest energies (See Figure 2) is caused by the synchrotron cooling of the secondary produced pions and muons. The critical energy of the

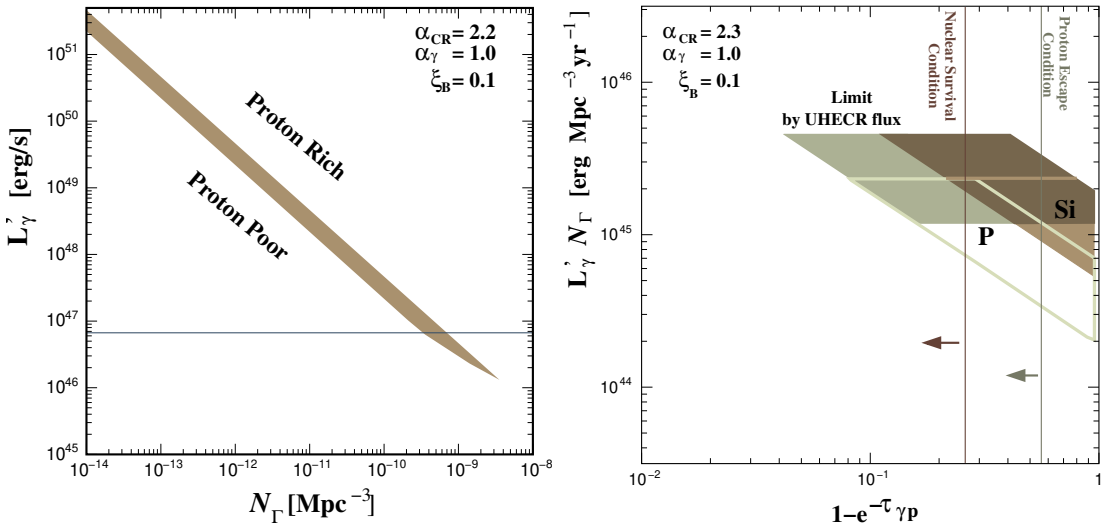

Figure 3. Left: The allowed region on the plane of the source luminosity L'_γ and the boosted source density $\mathcal{N}_\Gamma$. The parameters inside the shaded region meet the observational consistency criteria as in the left plot. The horizontal line shows the condition of Eq. (5). Right: The allowed region in the parameter space of luminosity per unit volume, $L'_\gamma \mathcal{N}_\Gamma$, and damping factor $1 - e^{-\tau_{p\gamma 0}}$. Any sources with the parameter values inside the shaded region can provide the UHECR and neutrino fluxes that are consistent with the observed data. The case of $\alpha_{\rm CR} = 2.2$ and $\alpha_\gamma = 1.0$ is shown. We find no Γ dependence on these constraints. The constraints for the silicon case is overlaid with the proton case for comparison. The constraints by the escape condition, Eq. (7), and by the nuclear survival condition, Eq. (9) are represented by the vertical lines. The horizontal belt displayed by the darker shade represents the systematics of UHECR energetics originating in the uncertainties on the mass composition and galactic to extra-galactic transition of UHECRs.

cooling is given by

$$\varepsilon^{\rm syn}_{\nu,\pi/\mu} \approx \Gamma \kappa_{\pi,\mu} \sqrt{\frac{6\pi}{\tau_{\pi,\mu}\sigma_T c B'^2} \frac{(m_{\pi/\mu}c^2)^5}{(m_e c^2)^2}}, \tag{14}$$

where $\kappa_{\pi,\mu}$ is the inelasticity from pion (muon) to a neutrino in the decay process. With Eq. (2), it is rewritten as

$$\varepsilon^{\rm syn}_{\nu,\pi/\mu} \approx \frac{\kappa_{\pi,\mu}}{\tau_{p\gamma 0}\Gamma} C(\alpha_\gamma, \tilde{\varepsilon}_0) \sqrt{\frac{L'_\gamma}{\xi_{\rm B}} \frac{6\pi}{\tau_{\pi,\mu}\sigma_T c} \frac{(m_{\pi/\mu}c^2)^5}{(m_e c^2)^2}}, \tag{15}$$

indicating that $\varepsilon^{\rm syn}_{\nu,\pi/\mu} \propto 1/(\tau_{p\gamma 0}\Gamma)$. This scaling plays a crucial role if the neutrino spectrum is harder like $\propto \varepsilon_\nu^{-1.8}$. The hardening is possible when the photon radiation spectrum is softer, as the neutrino spectrum follows $\sim \varepsilon_\nu^{-(\alpha_{\rm CR}-\alpha_\gamma+1)}$. As shown in the right panel of Figure 2, the spectral falloff below ~ 100 PeV is inevitable to be consistent with the EHE neutrino limit. The relativistic flow such as

$$\Gamma \gtrsim 20, \tag{16}$$

is, thus, required when the neutrino spectrum is harder than $\sim \varepsilon_\nu^{-1.8}$.

3. A new approach for finding the transient neutrino sources

The known source candidates to meet the conditions we discussed in the previous section are low-luminosity GRBs (LLGRBs) and low-luminosity tidal disruption events (LLTDEs). They can be powerful enough to accelerate heavy nuclei, though not protons, to UHE range along with

meeting the UHECR escape and survival requirements. The cosmic ray loading factor to meet the luminosity density requirement represented by Figure 3 and Eq. (13) is $\xi_{\rm CR} \simeq 10(\Gamma/3)^{-2}$ for LLGRBs and $\xi_{\rm CR} \simeq 100(\Gamma/10)^{-2}$ for LLTDEs. The detailed discussions are found in Ref. [8]. LLGRBs and LLTDEs are transient in optical/NIR and possibly X-ray bands. The obvious approach to identify them as neutrino sources is to run ToO observations by optical telescopes, triggered by neutrino detection alerts. However there are more than a hundred of supernovae (SNe) found in a 1 deg^2 sky patch in the optical sky. They mimic the transient neutrino sources and thus form a vast background in identifying the true neutrino counterpart. What is even worse is that LLGRBs might appear as engine-driven SNe, and a supernova out of the hundreds of SNe found in the sky can be a genuine UHECR/neutrino emitter. It is therefore very challenging to claim robust associations between a neutrino detection and its optical counterpart candidate.

We propose a new approach of the neutrino search to overcome this issue. That is to search for neutrino multiplets, two (doublet) or more neutrinos originating from the same direction within a time scale of $\Delta T \lesssim 30$ days [13], which is comparable to the time scale of neutrino flare expected in the neutrino source candidates. A given neutrino source must be in our neighborhood to yield a multiplet neutrino detection by a neutrino telescope with a size of ~ 1 km^3. All the SNe found at far distances away cannot be responsible for the multiplet signal and thus the optical follow-up observations triggered by a multiplet neutrino detection are not contaminated by unrelated SNe coincident detections if their redshift information is available.

3.1. Neutrino multiplet detection

The number of transient sources that could produce detectable neutrino multiplets for a given neutrino telescope is given by [14]

$$N^{\rm M}_{\Delta\Omega} = \frac{\Delta\Omega}{4\pi} \int_{z_{\rm min}}^{z_{\rm max}} dz d_z^2 (1+z) \left| \frac{dt}{dz} \right| P_{\rm p}^{n\geq 2}[\mu^{\rm s}(z)] n_0 \psi(z), \tag{17}$$

where $\Delta\Omega = 1$ deg^2 is the solid angle for a given direction of the neutrino multiplet and $P_{\rm p}^{n\geq 2}$ is the Poisson probability of producing multiple neutrinos for the mean number of neutrinos $\mu^{\rm s}$ from a source at redshift z. $\mu^{\rm s}(z)$ can be estimated for a given neutrino flux from a source at z assuming the multiplet search time window $T_{\rm w} = 30$ days which is long enough to contain the neutrino flare time scale ΔT. $N^{\rm M}_{\Delta\Omega}$ after the energy based cuts for filtering the atmospheric neutrino background contributions are shown in the left panel of Figure 4 [13].

The global rate of number of multiplet source in the 2π sky is converted from $N^{\rm M}_{\Delta\Omega}$ as

$$\begin{aligned} N^{\rm M}_{\rm all} &= \left(\frac{2\pi}{\Delta\Omega}\right)\left(\frac{T_{\rm obs}}{T_{\rm w}}\right) N^{\rm M}_{\Delta\Omega} \\ &\simeq 1.2 \left(\frac{T_{\rm obs}}{5\ {\rm yr}}\right)\left(\frac{N^{\rm M}_{\Delta\Omega}}{10^{-6}}\right). \end{aligned} \tag{18}$$

Hence, the parameter space of $N^{\rm M}_{\Delta\Omega} \gtrsim 10^{-6}$ is accessible by a 1 km^3 scale neutrino telescope. Any source candidate with the neutrino burst rate rarer than $\sim 10^{-7}$ Mpc^{-3} yr^{-1} are reachable by a few year observation with a 1 km^3 neutrino telescope. The detailed results are presented in Ref. [13].

3.2. A optical/NIR follow-up search strategy for identifying the optical counterpart

Among the counterpart candidates found in a ToO observation by a optical/NIR telescope triggered by a neutrino multiplet event detection, the nearest object is the most likely neutrino emitter. The pdf of the object with the minimum redshift, $z^{\rm trans}_{\rm min}$ is shown in the right panel of Figure 4, for the signal hypothesis and for the coincident SNe background hypothesis,

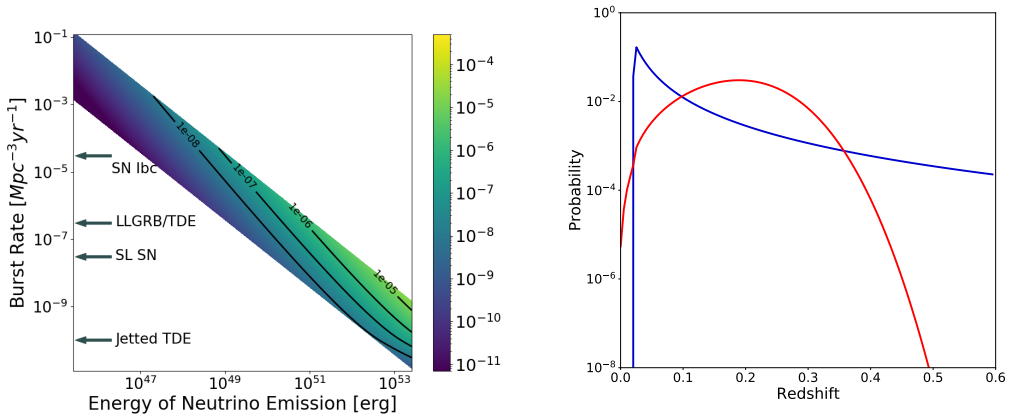

Figure 4. Left: Number of sources to yield neutrino multiplet, $N^{\rm M}_{\Delta\Omega}$, in $\Delta\Omega = 1$ deg^2 of sky on the parameter space of the output neutrino energy from a source and the burst density rate, after the cut to filter out the atmospheric neutrino contaminations [13]. The resultant annual false alarm rate ~ 0.25 for 2π sky. The expected ranges of the burst rate for several representative transient source candidates are also shown for reference. Right: Probability distribution of $z^{\rm trans}_{\rm min}$ as a function of redshift with bin size $\Delta z = 0.005$. The blue curve represents the case of the signal hypothesis, and the red curve shows the case of the coincident background hypothesis. $\mathcal{E}^{\rm fl}_{\nu} = 1 \times 10^{49}$ erg and $\rho_0 = 3 \times 10^{-6}$ Mpc^{-3} yr^{-1} are assumed for the multiplet source.

respectively. As they are quite different each other, we can statistically estimate p-value against the coincident background hypothesis, for a given $z^{\rm trans}_{\rm min}$. For example, finding an SN-like transient at z = 0.04 in an optical follow-up observation leads to $\sim 2.7\sigma$ significance against the background hypothesis. A several trials of the ToO observations will secure the firm detection of the counterpart objects, or place the substantial constraints on the source parameter space of the neutrino source emission energy and the burst rate density.

Acknowledgments

I am grateful to the CRIS 2022 organizers for their warm hospitality. Many of the results presented in this article have been obtained by the collaboration to publish the two papers [8, 13], and special thanks go to my coauthors of these publications, Kohta Murase, Masaomi Tanaka, Nobuhiro Shimizu, and Aya Ishihara.

References

[1] Waxman E and Bahcall J N 1999 *Phys. Rev. D* **59** 023002 (*Preprint* hep-ph/9807282)
[2] Murase K and Fukugita M 2019 *Phys. Rev. D* **99** 063012 (*Preprint* 1806.04194)
[3] Aartsen M G *et al.* (IceCube) 2021 *Nature* **591** 220–224
[4] Murase K, Kimura S S and Meszaros P 2020 *Phys. Rev. Lett.* **125** 011101 (*Preprint* 1904.04226)
[5] Aartsen M *et al.* (IceCube) 2016 *Phys. Rev. Lett.* **117** 241101 [Erratum: Phys.Rev.Lett. 119, 259902 (2017)] (*Preprint* 1607.05886)
[6] van Vliet A, Alves Batista R and Hörandel J R 2019 *Phys. Rev. D* **100** 021302 (*Preprint* 1901.01899)
[7] Fang K and Murase K 2018 *Nature Phys.* **14** 396–398 (*Preprint* 1704.00015)
[8] Yoshida S and Murase K 2020 *Phys. Rev. D* **102** 083023 (*Preprint* 2007.09276)
[9] Yoshida S and Takami H 2014 *Phys. Rev. D* **90** 123012 (*Preprint* 1409.2950)
[10] Aartsen M *et al.* (IceCube) 2015 *34th International Cosmic Ray Conference* (*Preprint* 1510.05223)
[11] Aartsen M *et al.* (IceCube) 2016 *Astrophys. J.* **833** 3 (*Preprint* 1607.08006)
[12] Aartsen M *et al.* (IceCube) 2018 *Phys. Rev. D* **98** 062003 (*Preprint* 1807.01820)
[13] Yoshida S, Murase K, Tanaka M, Shimizu N and Ishihara A 2022 *Astrophys. J.* **937** 108 (*Preprint* 2206.13719)
[14] Murase K and Waxman E 2016 *Phys. Rev. D* **94** 103006 (*Preprint* 1607.01601)